JOINT EUROPEAN TORUS

JET–P(93)43

G. Magyar, B. Denne-Hinnov, R. Giannella, N. Hawkes,
L. Lauro-Taroni, M. Matioli, D. Pasini

Injected Impurity Transport Diagnostic on JET

Injected Impurity Transport Diagnostic on JET

G. Magyar, B. Denne-Hinnov, R. Giannella, N. Hawkes,
L. Lauro-Taroni, M. Matioli, D. Pasini

JET-Joint Undertaking, Culham Science Centre, OX14 3DB, Abingdon, UK

Preprint of a paper presented to the KFA-IPP-KFKI Joint Workshop,
KFKI Research Institute, Budapest, 29 March - 2 April 1993
May 1993

INJECTED IMPURITY TRANSPORT DIAGNOSTIC ON JET

G Magyar
in collaboration with B Denne-Hinnov, R Giannella, N Hawkes,
L Lauro-Taroni, M Mattioli and D Pasini

JET Joint Undertaking, Abingdon, Oxon OX14 3EA, UK

1. BRIEF DESCRIPTION OF THE DIAGNOSTIC

JET is a large D-shaped tokamak with major radius R_0 = 2.96 m, minor radius a = 1.25 m, nominal toroidal field B_T = 3.4 T, plasma current I_P up to 7 MA and plasma elongation up to 1.6.

A schematic of the laser blow-off impurity injection system is shown in Fig.1

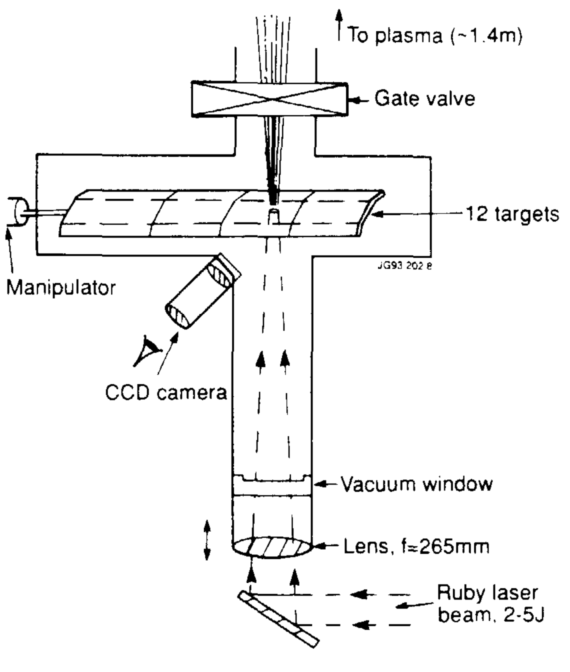

Figure 1. Schematic diagram of the diagnostic.

The target chamber which contains glass slide targets coated with various materials is attached to the bottom of the vacuum vessel. When the laser is fired onto the target it vaporizes from its surface the thin layer of coated material (5 μm thick) producing a burst of impurities which can propagate towards the plasma. All the material within the 3-4 mm spot size is evaporated which corresponds to a few 10^{18} atoms; of these, only a fraction reaches the plasma centre leading to impurity concentration of a few 10^{-4} n_e. The injected neutral particles have energies of the order of a few eV and reach the plasma boundary, 1.4 m away, in less than 1 ms. The atoms are ionized at the plasma edge and spread out rapidly along the field lines with toroidal velocity in the range of 10^4 m/s. At the same time, because of collisions or turbulence, the ions move slowly radially inwards with typical velocities of 1 to 10 m/s.

The progression of the impurities into the plasma is followed with good spatial and temporal resolution using two soft X-ray cameras. The system uses 38 viewing lines in a vertically oriented fan and 62 in a horizontal fan providing a spatial resolution of 7 cm and a time resolution of 5 μs. It is absolutely calibrated within 5% and allows tomographic reconstruction of the X-ray emission. Many absorption filters are available to study the emission in different energy bands. A 250μm Be filter was used in the present work which helped to discriminate the emission of the injected impurities from the background plasma emission

c) In fact, the N_{Ni} shows a random fluctuation by a factor 2-2.5 and independent from the main plasma parameters (plasma current, electron density and temperature, toroidal field, edge distance). See Fig.2. This fluctuation is most likely due to the non-uniform laser intensity ('hot spots'). This fluctuation makes it very difficult to find quantitative relationships with various parameters.

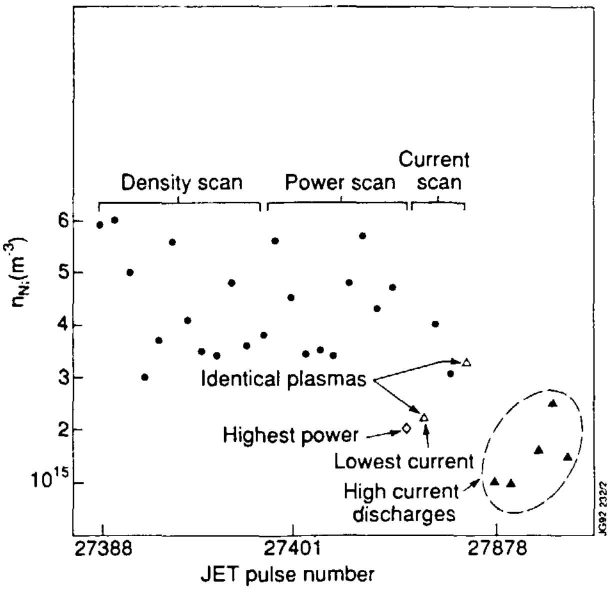

Figure 2. Possible correlations are masked by relatively large fluctuations of Ni concentration.

d) For such correlations we can use data from injection of Fe into X-point and H-mode plasmas. The inter-scenario comparison of Fe might be instructive and is shown in Figure 3. For relative comparisons, the number of counts, proportional to the intensity of the 192 Å line was used and normalised with the central electron density, $n_e(0)$. (The absolute density of Fe could be derived with the aid of transport codes.) Five different plasma scenarios were employed. In three of them there were sufficient number of similar discharges to show the fluctuation of the injected intensity by a factor of ~2, similarly to the Ni case. This implies that the fluctuation is not dependent on the ablated material.

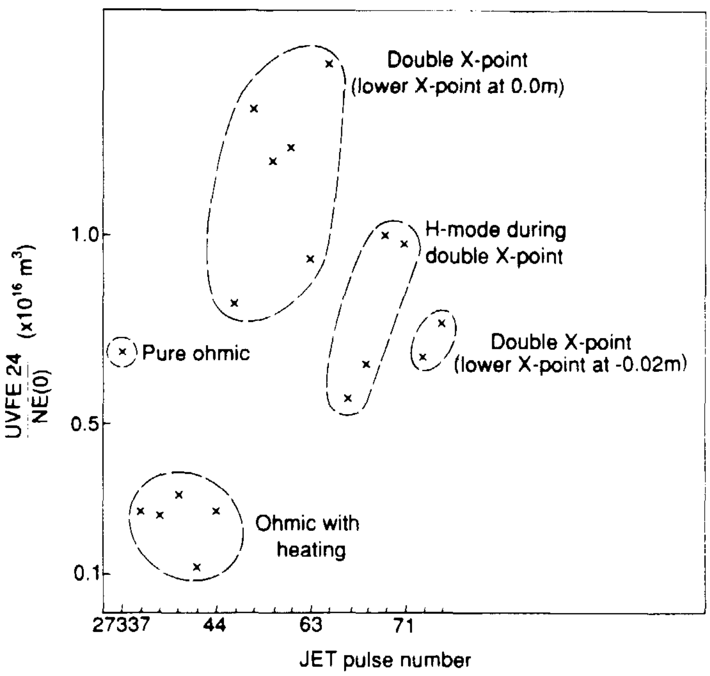

Figure 3. The concentration of Fe ions as a function of various plasma regimes.

The double X-point injections produced much higher intensities, by a factor of ~4 than the ohmically heated ones. The H-mode injections dropped somewhat in intensity by ~50%. Similar reduction resulted from the lowering of the X-point below the vessel wall by ~ 2 cm. The reduction in H-mode is observed quite generally, presumably due to the reduced transport.

3. REVIEW OF THE MAIN TRANSPORT RESULTS

Time or frequency measurements are more reliable, independent from the fluctuations of the impurity concentration.

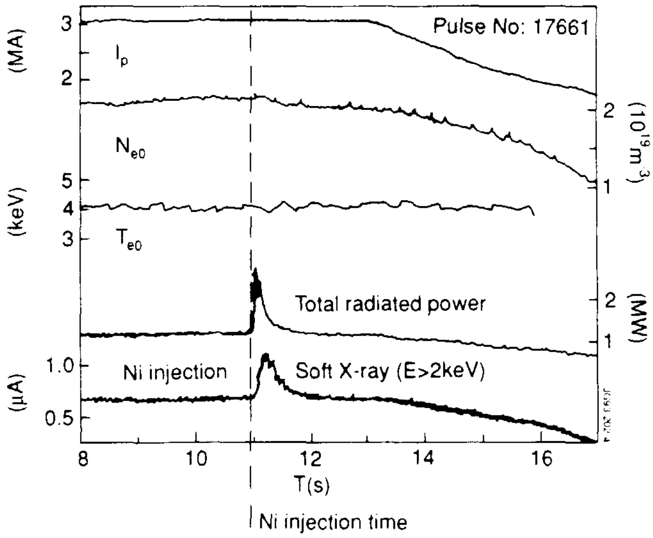

a) **Figure 5. The small quantity (~5 x 10^{-4} n_e) of injected impurity does not significantly perturb the main plasma parameters, i.e. the laser blow-off is a non-perturbing diagnostic.**

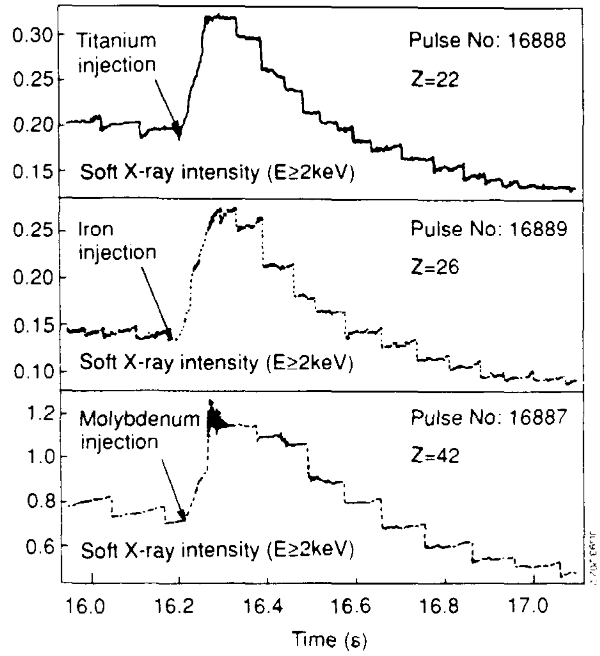

b) **Figure 6. No noticeable differences in transport are observed with the Z value of the injected impurity i.e.τ_{imp} is independent from the Z of impurity.**

The evolution of soft X-ray emissivity has been modelled with an impurity particle flux of the form:

$$\Gamma_{exp}=-D_{exp}\,\nabla n+V_{exp}\,n$$

where D_{exp} is the experimental diffusion coefficient and V_{exp} the experimental convective velocity

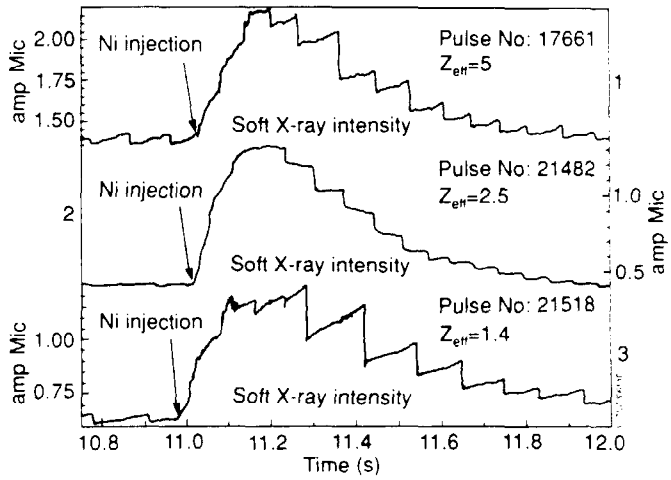

c) **Figure 7. No difference in impurity transport is observed with Zeff of the background plasma, i.e. τ_{imp} is independent from the Zeff of background plasma.**

h) The existence of a central low diffusivity region also explains:

- the persistance of a peaked distribution of pellet injected material.

- and the slow build-up of high ionization stage of eg Ni XXVI in the centre (~ 100 ms).

- The persistence of the peaked profiles (SXR and n_e) is a consequence of the low value of D in the central region.

- The Ni XXVI line rises more slowly during the H-mode indicating a smaller value of D in the plasma interior compared to L-mode.

See Figs.11 and 12.

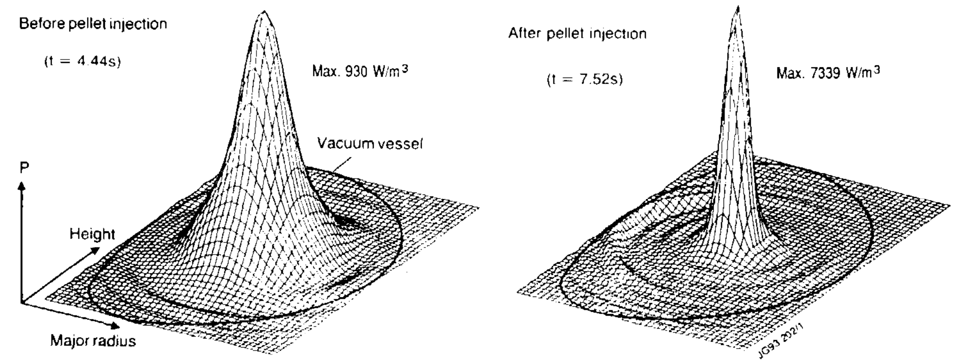

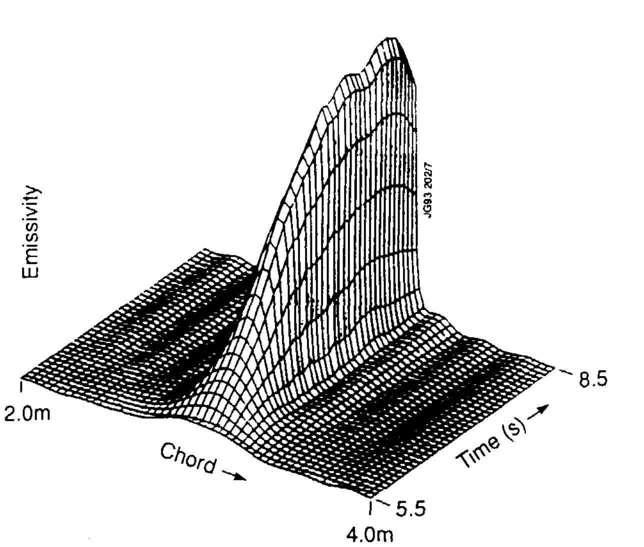

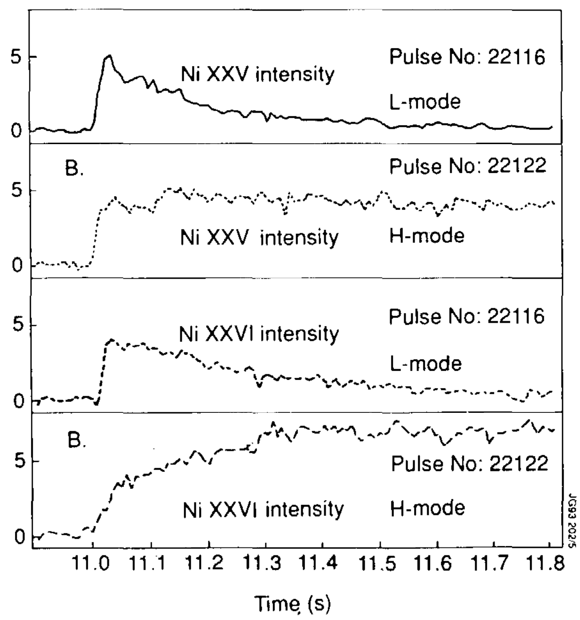

Figure 11. Peaked X-ray emissivity distribution following central pellet injection.

Figure 12. Time evolution of Ni XXV and Ni XXVI line intensities after Ni injection into L-mode and H-mode plasmas.

k) Scaling of impurity injection with various plasma parameters shows:

α) the size of the low diffusivity central region increases when q(a) is reduced due to either an increase in I_p or a reduction of B_T i.e. the central region becomes broader the flatter the q-profile (Fig.15).

β) τ_{imp} as given by the decay time of the central X-ray signal decreases as $P_{tot}/\langle n_e \rangle$ increases (Fig. 16).

γ) the larger $P_{tot}/\langle n_e \rangle$, implying larger T_e and ΔT_e, the larger is D in the outer region (Fig.17).

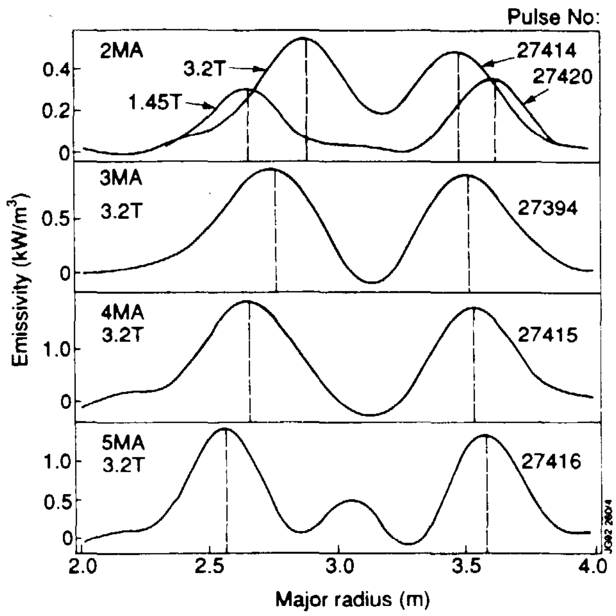

Fig. 15. X-ray emissivity profiles 70 ms after Ni injection (background emission subtracted).

δ) Density scan

At constant power increased $\langle n_e \rangle$ leads to increased τ_{imp}.
However T_e varies, too.
Choosing two pulses where the T_e profile was 'constant' but the n_e profile was different shows that τ_{imp} is the same, ie it does not depend on the density.

In fact, varying the total heating power or the average density, while keeping B_T and I_p constant, did not affect the dimension of the low diffusivity region.

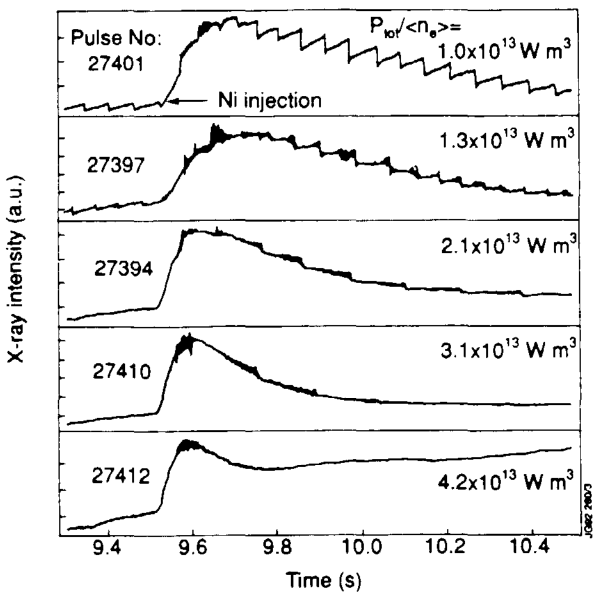

Figure 16. Evolution of the central chord X-ray intensity following Ni injection.

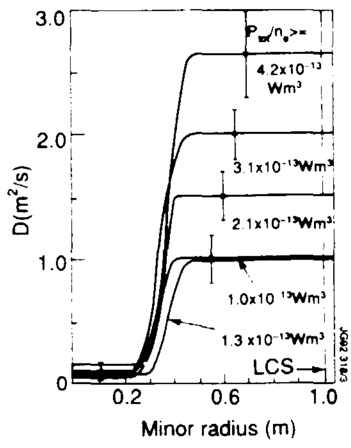

Figure 17. Ni diffusion coefficients for the plasma pulses shown above.